Thébault *et al. Earth, Planets and Space* (2015) 67:79
DOI 10.1186/s40623-015-0228-9

Earth, Planets and Space
a SpringerOpen Journal

LETTER Open Access

International Geomagnetic Reference Field: the 12th generation

Erwan Thébault[1*], Christopher C Finlay[2], Ciarán D Beggan[3], Patrick Alken[4,5], Julien Aubert[6], Olivier Barrois[7], Francois Bertrand[8,9], Tatiana Bondar[10], Axel Boness[8,9], Laura Brocco[6], Elisabeth Canet[11], Aude Chambodut[12], Arnaud Chulliat[4,5], Pierdavide Coïsson[6], François Civet[1], Aimin Du[13], Alexandre Fournier[6], Isabelle Fratter[14], Nicolas Gillet[7], Brian Hamilton[3], Mohamed Hamoudi[15,19], Gauthier Hulot[6], Thomas Jager[8,9], Monika Korte[15], Weijia Kuang[16], Xavier Lalanne[6], Benoit Langlais[1], Jean-Michel Léger[8,9], Vincent Lesur[15], Frank J Lowes[17], Susan Macmillan[3], Mioara Mandea[18], Chandrasekharan Manoj[4,5], Stefan Maus[4], Nils Olsen[2], Valeriy Petrov[10], Victoria Ridley[3], Martin Rother[15], Terence J Sabaka[16], Diana Saturnino[1], Reyko Schachtschneider[15], Olivier Sirol[6], Andrew Tangborn[20], Alan Thomson[3], Lars Tøffner-Clausen[2], Pierre Vigneron[6], Ingo Wardinski[15] and Tatiana Zvereva[10]

Abstract

The 12th generation of the International Geomagnetic Reference Field (IGRF) was adopted in December 2014 by the Working Group V-MOD appointed by the International Association of Geomagnetism and Aeronomy (IAGA). It updates the previous IGRF generation with a definitive main field model for epoch 2010.0, a main field model for epoch 2015.0, and a linear annual predictive secular variation model for 2015.0-2020.0. Here, we present the equations defining the IGRF model, provide the spherical harmonic coefficients, and provide maps of the magnetic declination, inclination, and total intensity for epoch 2015.0 and their predicted rates of change for 2015.0-2020.0. We also update the magnetic pole positions and discuss briefly the latest changes and possible future trends of the Earth's magnetic field.

Keywords: Geomagnetism; Field modeling; IGRF

Correspondence/Findings

Introduction

The International Geomagnetic Reference Field (IGRF) is a series of mathematical models describing the large-scale internal part of the Earth's magnetic field between epochs 1900 A.D. and the present. The IGRF has been maintained and produced by an international team of scientists under the auspices of the International Association of Geomagnetism and Aeronomy (IAGA) since 1965 (Zmuda 1971). It results from a collaborative effort between magnetic field modelers and institutes involved in collecting and disseminating magnetic field data from magnetic observatories (see the Appendix for the list of World Data Centers), ground surveys, and low Earth orbiting (LEO) satellites. The IGRF is used by scientists in a wide variety of studies, for instance, concerning the dynamics of the Earth's core field, space weather, or local magnetic anomalies imprinted in the Earth's crust. It is also used by commercial organizations and individuals as a source of orientation information.

The IGRF model must be regularly revised in order to follow the continuous temporal changes of the geomagnetic field generated in the Earth's outer core. The period between revisions is however sufficiently short to preserve its utility as a reference model in applications requiring a fixed reference standard. Table 1 provides the nomenclature and a summary of the history of previous generations of the IGRF. At present, each generation consists of three constituent models. One constituent is designated a Definitive Geomagnetic Reference Field (DGRF). The term 'definitive' is used because any further improvement of these retrospectively determined models is unlikely. The second constituent model, referred to as

*Correspondence: erwan.thebault@univ-nantes.fr
[1]Laboratoire de Planétologie et Géodynamique de Nantes, University of Nantes, UMR 6112 CNRS, 1 chemin de la Houssiniére F-44322, Nantes, France
Full list of author information is available at the end of the article

Table 1 Summary of IGRF generations, their intervals of validity, and related references

Full name	Short name	Valid for	Definitive for	Reference
IGRF 12th generation	IGRF-12	1900.0-2020.0	1945.0-2010.0	Thébault et al., this article
IGRF 11th generation	IGRF-11	1900.0-2015.0	1945.0-2005.0	Finlay et al. (2010a)
IGRF 10th generation	IGRF-10	1900.0-2010.0	1945.0-2000.0	Maus et al. (2005)
IGRF 9th generation	IGRF-9	1900.0-2005.0	1945.0-2000.0	Macmillan et al. (2003)
IGRF 8th generation	IGRF-8	1900.0-2005.0	1945.0-1990.0	Mandea and Macmillan (2000)
IGRF 7th generation	IGRF-7	1900.0-2000.0	1945.0-1990.0	Barton (1997)
IGRF 6th generation	IGRF-6	1945.0-1995.0	1945.0-1985.0	Langel (1992)
IGRF 5th generation	IGRF-5	1945.0-1990.0	1945.0-1980.0	Langel et al. (1988)
IGRF 4th generation	IGRF-4	1945.0-1990.0	1965.0-1980.0	Barraclough (1987)
IGRF 3rd generation	IGRF-3	1965.0-1985.0	1965.0-1975.0	Peddie (1982)
IGRF 2nd generation	IGRF-2	1955.0-1980.0	–	IAGA (1975)
IGRF 1st generation	IGRF-1	1955.0-1975.0	–	Zmuda (1971)

an IGRF model, is non-definitive - it will eventually be replaced by a definitive model in a future revision of the IGRF. The final constituent, referred to as the secular variation (SV), is provided to predict the time variation of the large-scale geomagnetic field for the 5 years following the latest revision of the IGRF. Readers interested in the history of the IGRF should consult Barton (1997), and users can find legacy versions of the IGRF at the online archive located at http://www.ngdc.noaa.gov/IAGA/vmod/igrf_old_models.html. These may prove useful for those wishing to recover data from which a previous generation of the IGRF has been subtracted or who wish to use the latest generation of the IGRF to carry out revised analyses. Here, attention will focus on the most recent 12th-generation IGRF, hereafter referred to as IGRF-12, that provides a DGRF model for epoch 2010.0, an IGRF model for epoch 2015.0, and a predictive SV model covering the epochs 2015.0-2020.0. IGRF-12 was agreed in December 2014 by a task force of the IAGA Working Group V-MOD. The purpose of this note is to document the release of IGRF-12, to act as a permanent published record of the IGRF-12 set of model coefficients, and to briefly describe some major features of the geomagnetic field at the Earth's surface as revealed by the updated model.

Mathematical formulation of the IGRF model

The IGRF is a series of mathematical models of the internal geomagnetic field $\overrightarrow{B}(r,\theta,\phi,t)$ and its annual rate of change (secular variation). On and above the Earth's surface, the magnetic field $\overrightarrow{B}$ is defined in terms of a magnetic scalar potential V by $\overrightarrow{B} = -\nabla V$ and where in spherical polar co-ordinates V is approximated by the finite series

$$V(r,\theta,\phi,t) = a\sum_{n=1}^{N}\sum_{m=0}^{n}\left(\frac{a}{r}\right)^{n+1} \times \left[g_n^m(t)\cos(m\phi) + h_n^m(t)\sin(m\phi)\, P_n^m(\cos\theta)\right], \tag{1}$$

with r denoting the radial distance from the center of the Earth, $a = 6,371.2$ km being the geomagnetic conventional Earth's mean reference spherical radius, θ denoting geocentric co-latitude, and ϕ denoting east longitude. The functions $P_n^m(\cos\theta)$ are the Schmidt quasi-normalized associated Legendre functions of degree n and order m. The Gauss coefficients g_n^m, h_n^m are functions of time and are conventionally given in units of nanotesla (nT).

In the IGRF-12 model, the Gauss coefficients g_n^m and h_n^m are provided for the main field (MF) at epochs separated by 5 years between 1900.0 and 2015.0 A.D. The time dependence of the Gauss coefficients is assumed to be linear over 5-year intervals and is specified by the following expression

$$g_n^m(t) = g_n^m(T_0) + \dot{g}_n^m(T_0).(t - T_0), \tag{2}$$

$$h_n^m(t) = h_n^m(T_0) + \dot{h}_n^m(T_0).(t - T_0), \tag{3}$$

where $\dot{g}_n^m$ $\left(\text{respectively } \dot{h}_n^m\right)$ given in units of nT/year represent the 5-year average first time derivative (the linear secular variation) of the Gauss coefficients. t is the time of interest in units of year and T_0 is the epoch preceding t which is an exact multiple of 5 years, such that $T_0 \leq t < (T_0 + 5.0)$. When MF models exist for both T_0 and $T_0 + 5.0$, then coefficients $\dot{g}_n^m(T_0)$ can be computed as $[g_n^m(T_0 + 5.0) - g_n^m(T_0)]/5.0$. For the final 5 years of the model validity (between 2015.0 and 2020.0 for IGRF-12),

Table 2 Magnetic observatories contributing data used in the construction of IGRF-12

Supporting Agencies	Country	Observatory IAGA code
Centre de Recherche en Astronomie, Astrophysique et Geophysique	Algeria	TAM
Universidad Nacional de la Plata	Argentina	TRW
Servicio Meteorologico Nacional	Argentina	ORC
Geoscience Australia	Australia	ASP, CKI, CNB, CSY, CTA, DVS, GNA, GNG, KDU, LRM, MAW, MCQ
Zentralanstalt für Meteorologie und Geodynamik	Austria	WIK
Institut Royal Météorologique	Belgium	DOU, MAB
CNPq-Observatorio Nacional	Brazil	VSS
Academy of Sciences	Bulgaria	PAG
Geological Survey of Canada	Canada	ALE, BLC, CBB, FCC, IQA, MEA, OTT, PBQ, RES, STJ, VIC,YKC
Centro Meteorológico Regional Pacifico	Chile	IPM
Academy of Sciences	China	BMT
China Earthquake Adminstration	China	CDP, GLM, GZH, KSH, LZH, MZL, QGZ, QIX, QZH, SSH, THJ, WHN
Academy of Sciences	Czech Republic	BDV
Danish Technical University-Space	Denmark	TDC
Addis Ababa University	Ethiopia	AAE
Finnish Meteorological Institute	Finland	NUR
Geophysical Observatory	Finland	SOD
Institut de Physique du Globe de Paris	France	AAE, BOX, CLF, KOU, IPM, LZH, MBO, PHU, QSB, PPT, TAM
Ecole et Observatoire des Sciences de la Terre	France	AMS, CZT, DMC, DRV, PAF, TAN
Institut Français de Recherche Scientifique pour le Développement	France	BNG, MBO
Academy of Sciences	Georgia	TFS
Universität München	Germany	FUR
Alfred-Wegener-Institute for Polar Marine Research	Germany	VNA
GFZ Hemholtz Centre Potsdam	Germany	NGK, TDC, WNG
Universität Stuttgart	Germany	BFO
Institute of Geology and Mineral Exploration	Greece	PEG
Academy of Sciences	Hungary	NCK
Eötvös Loránd Geophysical Institute	Hungary	THY
University of Iceland	Iceland	LRV
Indian Institute of Geomagnetism	India	ABG, PND, SIL, TIR, VSK
National Geophysical Research Institute	India	HYB
Meteorological and Geophysical Agency	Indonesia	KPG, PLR, TND
Meteorological Service	Ireland	VAL
Survey of Israel	Israel	AMT, BGY, ELT
Instituto Nazionale di Geofisica e Vulcanologia	Italy	AQU, DMC
Japan Coast Guard	Japan	HTY
Japan Meteorological Agency	Japan	CBI, KAK, KNY, MMB
Geographical Survey Institute	Japan	ESA, KNZ, MIZ
Institute of the Ionosphere	Kazakhstan	AAA

Table 2 Magnetic observatories contributing data used in the construction of IGRF-12 *(Continued)*

National Centre for Geophysical Research	Lebanon	QSB
Université d'Antananarivo	Madagascar	TAN
Gan Meteorological Office/ETH Zurich	Maldives/Switzerland	GAN
Universidad Nacional Autonoma de México	Mexico	TEO
Institute of Geological and Nuclear Sciences	New Zealand	API, EYR, SBA
University of Tromsø	Norway	BJN, DOB, TRO
Instituto Geofisico del Peru	Peru	HUA
Academy of Sciences	Poland	BEL, HLP, HRN
Directorate General of Telecommunications	Republic of China	LNP
Instituto Nacional de Geologia	República de Moçambique	LMM
Geological Survey of Romania	Romania	SUA
Academy of Sciences	Russia	ARS, BOX, LVV, MOS, NVS
Institute of Solar-Terrestrial Physics	Russia	IRT
Dept. of Agriculture, Forestry, Fisheries & Meteorology	Samoa	API
Geomagnetic College Grocka	Serbia and Montenegro	GCK
Slovenska Akademia Vied	Slovakia	HRB
National Research Foundation	South Africa	HBK, HER, KMH, TSU
Observatori de l'Ebre	Spain	EBR, LIV
Real Instituto y Observatorio de la Armada	Spain	SFS
Instituto Geográfico Nacional	Spain	GUI, SPT
Sveriges Geologiska Undersökning	Sweden	ABK, LOV, LYC, UPS
Swedish Institute of Space Physics	Sweden	KIR
Bŏgaziçi University	Turkey	IZN
Academy of Sciences	Ukraine	AIA
British Geological Survey	United Kingdom	ASC, ESK, HAD, JCO, KEP, LER, PST, SBL
US Geological Survey	United States	BRW, BOU, BSL, CMO, DLR, FRD, FRN, GUA HON, NEW, SIT, SJG, SHU, TUC
Academy of Science and Technology	Vietnam	PHU

the coefficients $\dot{g}_n^m(t)$ and $\dot{h}_n^m(t)$ of the predictive average SV are explicitly provided. The geocentric components of the geomagnetic field in the northward, eastward, and radially inwards directions (X, Y and Z) are obtained from the model coefficients using Equation 1 and by taking the gradient of V in spherical polar co-ordinates

$$X = \frac{1}{r}\frac{\partial V}{\partial \theta}, \quad Y = -\frac{1}{r\sin\theta}\frac{\partial V}{\partial \phi}, \quad Z = \frac{\partial V}{\partial r}. \tag{4}$$

For some applications, the declination D, the inclination I, the horizontal intensity H, and the total intensity F are required. These components are calculated from X, Y, and Z using the relations,

$$\begin{aligned} H &= \sqrt{X^2+Y^2}, \quad F = \sqrt{X^2+Y^2+Z^2}, \\ D &= \arctan{(Y/X)}, \quad I = \arctan{(Z/H)}. \end{aligned} \tag{5}$$

In Equation 1, the maximum spherical harmonic degree of the expansion N may vary from one epoch to another. The maximum degree N of the series is equal to 10 up to and including epoch 1995.0 and the coefficients are quoted to 1-nT precision. For epoch 2000, the coefficients are provided to degree and order 13 and quoted to 0.1-nT precision, and from epoch 2005 onwards they are quoted to 0.01-nT precision for the DGRF (and 0.1 nT for the latest non-definitive IGRF), to take advantage of the higher data quality and good coverage provided by the LEO satellite missions (Finlay et al. 2010a). The maximum truncation degree $N = 13$ for epochs after 2000 is defined so as not to include the crustal magnetic field contributions that dominate at higher degrees (see e.g., Langel and Estes 1982).

The predictive SV coefficients $\dot{g}_n^m(t)$ and $\dot{h}_n^m(t)$ are given to degree and order 8 to 0.1-nT/year precision. Because of these changes in precision and nomenclature, it is recommended to always use the term 'IGRF-gg,' where gg represents the generation, in order to keep track of the coefficients that were actually used in applications. This is a simple way to standardize studies carried out at different epochs that makes it apparent whether the results are 'predictive' and therefore less accurate or 'definitive'. For example, one cannot recover the original full-field measurement from an aeromagnetic anomaly map if one does not know which generation of the IGRF was used. This issue has important consequences when comparing magnetic surveys carried out at different epochs (e.g., Hamoudi et al. 2007; Hemant et al. 2007; Maus et al. 2007).

Equation 1 is expressed in the geocentric system of co-ordinates, but it is sometimes necessary to work in geodetic co-ordinates. When converting between geocentric and geodetic co-ordinates (see for instance Hulot et al. 2007), it is recommended to use the World Geodetic System 1984 (WGS84) datum as present-day satellite magnetic data are often positioned using it. The WGS84 spheroid is defined with major (equatorial) radius $A =$ 6,378.137 km at the equator and a reciprocal flattening $f =$ 1/298.257223563 (the polar semi-minor axis is therefore $B = A(1-f) \simeq 6{,}356.752$ km).

The 12th-generation IGRF

IGRF-12, the 12th generation of IGRF, is derived from candidate models prepared by international teams who answered a call issued by the IGRF-12 task force in May 2014. This call requested candidates for the Definitive Geomagnetic Reference Field (DGRF) for epoch 2010, for a provisional IGRF model for epoch 2015, and for a predictive SV model for the interval 2015.0-2020.0. The IGRF-12 model coefficients remain unchanged for epoch 2005 and earlier.

The number of institutions participating in IGRF-12 was larger than for any previous generation. This reflects the constructive effect of open and unconditional cooperation between scientists involved in modeling the magnetic field, the institutions archiving and disseminating the ground magnetic data, and the national and the European space agencies who actively worked to distribute their expertise, computer programs, and magnetic satellite data with documentation. This latter point was especially important for the MF for epoch 2015.0 given the short period that elapsed between the launch of the Swarm satellites (in November 2013) and the submission of IGRF candidate models by October 2014. The European Space Agency provided prompt access to the Swarm satellite measurements, including detailed documentation and information on the operational status of the instruments (https://earth.esa.int/web/guest/missions/esa-operational-eo-missions/swarm). This allowed the teams producing candidate models to rapidly use the Swarm data and helped IGRF-12 to be delivered on time. The collection of ground-based magnetic observatory measurements (see Table 2) and the availability of other satellite measurements, from the CHAMP (Reigber et al. 2002), Ørsted (Neubert et al. 2001) and SAC-C missions, were also crucial for IGRF-12.

Seven candidate MF models for the DGRF epoch 2010.0 and ten candidate MF models for the IGRF epoch 2015.0 were submitted. In addition, nine SV models were submitted for the predictive part covering epochs 2015.0-2020.0. Team A was from BGS, UK (Hamilton et al. 2015); team B was from DTU Space, Denmark (Finlay et al. 2015); team C was led by ISTerre, France, with input from DTU Space (Gillet et al. 2015); team D was from IZMIRAN, Russia; team E was from NGDC/NOAA (Alken et al. 2015); team F was from GFZ, Germany (Lesur et al. 2015); team G was led by GSFC-NASA, USA, in collaboration with UMBC; team H was from IPGP (Fournier et al. 2015; Vigneron et al. 2015), France, in collaboration with the CEA-Léti (Léger et al. 2015) and with input from LPG Nantes and CNES, France; team I was led by LPG Nantes, France (Saturnino et al. 2015) with input from CNES; team J was from ETH Zurich, Switzerland. These teams contributed to all or parts of the three model constituents of IGRF. Following the IGRF specifications, the MF candidate models had a maximum spherical harmonic degree $N = 13$ and the predictive SV model had a maximum spherical harmonic degree $N = 8$.

The final IGRF-12 MF models for epochs 2010.0 and 2015.0 as well as the predictive SV model for 2015.0-2020.0 were calculated using a new weighting scheme of the candidate models. For the previous generation of IGRF, fixed weights were assigned to each candidate model based on information gleaned from the evaluations (see Finlay et al. 2010b, for instance) and most weight was given to those models showing the smallest scatter about the arithmetic mean of the candidate models. For IGRF-12, the evidence for significant systematic errors in one or more models was not thought to be sufficient to reject any of the models. A robust weighting scheme was instead applied to the candidate models in space, as agreed by a vote of the IGRF-12 task force. The specification of the candidate models and details of the evaluations and weighting scheme are described in a dedicated paper in this special issue (Thébault et al. 2015).

IGRF-12 model coefficients and maps

Table 3 lists the Schmidt semi-normalized spherical harmonic coefficients defining IGRF-12. In IGRF-12, only coefficients after epoch 2005.0 are modified, but all coefficients are included to serve as a complete record of the model since 1900. This should help to avoid any confusion with previous generations of IGRF, particularly with their provisional parts. The coefficients are given in units of nT

Table 3 **12th Generation International Geomagnetic Reference Field**

	Degree	Order	IGRF	IGRF	IGRF	IGRF	IGRF	IGRF	IGRF	IGRF	IGRF	DGRF	DGRF	DGRF	DGRF	DGRF	DGRF	DGRF	DGRF	DGRF	DGRF	DGRF	DGRF	DGRF	DGRF	IGRF	SV
g/h	n	m	1900.0	1905.0	1910.0	1915.0	1920.0	1925.0	1930.0	1935.0	1940.0	1945.0	1950.0	1955.0	1960.0	1965.0	1970.0	1975.0	1980.0	1985.0	1990.0	1995.0	2000.0	2005.0	2010.0	2015	2015-20
g	1	0	-31543	-31464	-31354	-31212	-31060	-30926	-30805	-30715	-30654	-30594	-30554	-30500	-30421	-30334	-30220	-30100	-29992	-29873	-29775	-29692	-29619.4	-29554.63	-29496.57	-29442.0	10.3
g	1	1	-2298	-2298	-2297	-2306	-2317	-2318	-2316	-2306	-2292	-2285	-2250	-2215	-2169	-2119	-2068	-2013	-1956	-1905	-1848	-1784	-1728.2	-1669.05	-1586.42	-1501.0	18.1
h	1	1	5922	5909	5898	5875	5845	5817	5808	5812	5821	5810	5815	5820	5791	5776	5737	5675	5604	5500	5406	5306	5186.1	5077.99	4944.26	4797.1	-26.6
g	2	0	-677	-728	-769	-802	-839	-893	-951	-1018	-1106	-1244	-1341	-1440	-1555	-1662	-1781	-1902	-1997	-2072	-2131	-2200	-2267.7	-2337.24	-2396.06	-2445.1	-8.7
g	2	1	2905	2928	2948	2956	2959	2969	2980	2984	2981	2990	2998	3003	3002	2997	3000	3010	3027	3044	3059	3070	3068.4	3047.69	3026.34	3012.9	-3.3
h	2	1	-1061	-1086	-1128	-1191	-1259	-1334	-1424	-1520	-1614	-1702	-1810	-1898	-1967	-2016	-2047	-2067	-2129	-2197	-2279	-2366	-2481.6	-2594.50	-2708.54	-2845.6	-27.4
g	2	2	924	1041	1176	1309	1407	1471	1517	1550	1566	1578	1576	1581	1590	1594	1611	1632	1663	1687	1686	1681	1670.9	1657.76	1668.17	1676.7	2.1
h	2	2	1121	1065	1000	917	823	728	644	586	528	477	381	291	206	114	25	-68	-200	-306	-373	-413	-458.0	-515.43	-575.73	-641.9	-14.1
g	3	0	1022	1037	1058	1084	1111	1140	1172	1206	1240	1282	1297	1302	1302	1297	1287	1276	1281	1296	1314	1335	1339.6	1336.30	1339.85	1350.7	3.4
g	3	1	-1469	-1494	-1524	-1559	-1600	-1645	-1692	-1740	-1790	-1834	-1889	-1944	-1992	-2038	-2091	-2144	-2180	-2208	-2239	-2267	-2288.0	-2305.83	-2326.54	-2352.3	-5.5
h	3	1	-330	-357	-389	-421	-445	-462	-480	-494	-499	-499	-476	-462	-414	-404	-366	-333	-336	-310	-284	-262	-227.6	-198.86	-160.40	-115.3	8.2
g	3	2	1256	1239	1223	1212	1205	1202	1205	1215	1232	1255	1274	1288	1289	1292	1278	1260	1251	1247	1248	1249	1252.1	1246.39	1232.10	1225.6	-0.7
h	3	2	3	34	62	84	103	119	133	146	163	186	206	216	224	240	251	262	271	284	293	302	293.4	269.72	251.75	244.9	-0.4
g	3	3	572	635	705	778	839	881	907	918	916	913	896	882	878	856	838	830	833	829	802	759	714.5	672.51	633.73	582.0	-10.1
h	3	3	523	480	425	360	293	229	166	101	43	-11	-46	-83	-130	-165	-196	-223	-252	-297	-352	-427	-491.1	-524.72	-537.03	-538.4	1.8
g	4	0	876	880	884	887	889	891	896	903	914	944	954	958	957	957	952	946	938	936	939	940	932.3	920.55	912.66	907.6	-0.7
g	4	1	628	643	660	678	695	711	727	744	762	776	792	796	800	804	800	791	782	780	780	780	786.8	797.96	808.97	813.7	0.2
h	4	1	195	203	211	218	220	216	205	188	169	144	136	133	135	148	167	191	212	232	247	262	272.6	282.07	286.48	283.3	-1.3
g	4	2	660	653	644	631	616	601	584	565	550	544	528	510	504	479	461	438	398	361	325	290	250.0	210.65	166.58	120.4	-9.1
h	4	2	-69	-77	-90	-109	-134	-163	-195	-226	-252	-276	-278	-274	-278	-269	-266	-265	-257	-249	-240	-236	-231.9	-225.23	-211.03	-188.7	5.3
g	4	3	-361	-380	-400	-416	-424	-426	-422	-415	-405	-421	-408	-397	-394	-390	-395	-405	-419	-424	-423	-418	-403.0	-379.86	-356.83	-334.9	4.1
h	4	3	-210	-201	-189	-173	-153	-130	-109	-90	-72	-55	-37	-23	3	13	26	39	53	69	84	97	119.8	145.15	164.46	180.9	2.9
g	4	4	134	146	160	178	199	217	234	249	265	304	303	290	269	252	234	216	199	170	141	122	111.3	100.00	89.40	70.4	-4.3
h	4	4	-75	-65	-55	-51	-57	-70	-90	-114	-141	-178	-210	-230	-255	-269	-279	-288	-297	-297	-299	-306	-303.8	-305.36	-309.72	-329.5	-5.2
g	5	0	-184	-192	-201	-211	-221	-230	-237	-241	-241	-253	-240	-229	-222	-219	-216	-218	-218	-214	-214	-214	-218.8	-227.00	-230.87	-232.6	-0.2
g	5	1	328	328	327	327	326	326	327	329	334	346	349	360	362	358	359	356	357	355	353	352	351.4	354.41	357.29	360.1	0.5
h	5	1	-210	-193	-172	-148	-122	-96	-72	-51	-33	-12	3	15	16	19	26	31	46	47	46	46	43.8	42.72	44.58	47.3	0.6
g	5	2	264	259	253	245	236	226	218	211	208	194	211	230	242	254	262	264	261	253	245	235	222.3	208.95	200.26	192.4	-1.3
h	5	2	53	56	57	58	58	58	60	64	71	95	103	110	125	128	139	148	150	150	154	165	171.9	180.25	189.01	197.0	1.7

Table 3 12th Generation International Geomagnetic Reference Field *(Continued)*

g	5	3	5	-1	-9	-16	-23	-28	-32	-33	-33	-20	-20	-23	-26	-31	-42	-59	-74	-93	-109	-118	-130.4	-136.54	-141.05	-140.9	-0.1
h	5	3	-33	-32	-33	-34	-38	-44	-53	-64	-75	-67	-87	-98	-117	-126	-139	-152	-151	-154	-153	-143	-133.1	-123.45	-118.06	-119.3	-1.2
g	5	4	-86	-93	-102	-111	-119	-125	-131	-136	-141	-142	-147	-152	-156	-157	-160	-159	-162	-164	-165	-166	-168.6	-168.05	-163.17	-157.5	1.4
h	5	4	-124	-125	-126	-126	-125	-122	-118	-115	-113	-119	-122	-121	-114	-97	-91	-83	-78	-75	-69	-55	-39.3	-19.57	-0.01	16.0	3.4
g	5	5	-16	-26	-38	-51	-62	-69	-74	-76	-76	-82	-76	-69	-63	-62	-56	-49	-48	-46	-36	-17	-12.9	-13.55	-8.03	4.1	3.9
h	5	5	3	11	21	32	43	51	58	64	69	82	80	78	81	81	83	88	92	95	97	107	106.3	103.85	101.04	100.2	0.0
g	6	0	63	62	62	61	61	61	60	59	57	59	54	47	46	45	43	45	48	53	61	68	72.3	73.60	72.78	70.0	-0.3
g	6	1	61	60	58	57	55	54	53	53	54	57	57	57	58	61	64	66	66	65	65	67	68.2	69.56	68.69	67.7	-0.1
h	6	1	-9	-7	-5	-2	0	3	4	4	4	6	-1	-9	-10	-11	-12	-13	-15	-16	-16	-17	-17.4	-20.33	-20.90	-20.8	0.0
g	6	2	-11	-11	-11	-10	-10	-9	-9	-8	-7	6	4	3	1	8	15	28	42	51	59	68	74.2	76.74	75.92	72.7	-0.7
h	6	2	83	86	89	93	96	99	102	104	105	100	99	96	99	100	100	99	93	88	82	72	63.7	54.75	44.18	33.2	-2.1
g	6	3	-217	-221	-224	-228	-233	-238	-242	-246	-249	-246	-247	-247	-237	-228	-212	-198	-192	-185	-178	-170	-160.9	-151.34	-141.40	-129.9	2.1
h	6	3	2	4	5	8	11	14	19	25	33	16	33	48	60	68	72	75	71	69	69	67	65.1	63.63	61.54	58.9	-0.7
g	6	4	-58	-57	-54	-51	-46	-40	-32	-25	-18	-25	-16	-8	-1	4	2	1	4	4	3	-1	-5.9	-14.58	-22.83	-28.9	-1.2
h	6	4	-35	-32	-29	-26	-22	-18	-16	-15	-15	-9	-12	-16	-20	-32	-37	-41	-43	-48	-52	-58	-61.2	-63.53	-66.26	-66.7	0.2
g	6	5	59	57	54	49	44	39	32	25	18	21	12	7	-2	1	3	6	14	16	18	19	16.9	14.58	13.10	13.2	0.3
h	6	5	36	32	28	23	18	13	8	4	0	-16	-12	-12	-11	-8	-6	-4	-2	-1	1	1	0.7	0.24	3.02	7.3	0.9
g	6	6	-90	-92	-95	-98	-101	-103	-104	-106	-107	-104	-105	-107	-113	-111	-112	-111	-108	-102	-96	-93	-90.4	-86.36	-78.09	-70.9	1.6
h	6	6	-69	-67	-65	-62	-57	-52	-46	-40	-33	-39	-30	-24	-17	-7	1	11	17	21	24	36	43.8	50.94	55.40	62.6	1.0
g	7	0	70	70	71	72	73	73	74	74	74	70	65	65	67	75	72	71	72	74	77	77	79.0	79.88	80.44	81.6	0.3
g	7	1	-55	-54	-54	-54	-54	-54	-54	-53	-53	-40	-55	-56	-56	-57	-57	-56	-59	-62	-64	-72	-74.0	-74.46	-75.00	-76.1	-0.2
h	7	1	-45	-46	-47	-48	-49	-50	-51	-52	-52	-45	-35	-50	-55	-61	-70	-77	-82	-83	-80	-69	-64.6	-61.14	-57.80	-54.1	0.8
g	7	2	0	0	1	2	2	3	4	4	4	0	2	2	5	4	1	1	2	3	2	1	0.0	-1.65	-4.55	-6.8	-0.5
h	7	2	-13	-14	-14	-14	-14	-14	-15	-17	-18	-18	-17	-24	-28	-27	-27	-26	-27	-27	-26	-25	-24.2	-22.57	-21.20	-19.5	0.4
g	7	3	34	33	32	31	29	27	25	23	20	0	1	10	15	13	14	16	21	24	26	28	33.3	38.73	45.24	51.8	1.3
h	7	3	-10	-11	-12	-12	-13	-14	-14	-14	-14	2	0	-4	-6	-2	-4	-5	-5	-2	0	4	6.2	6.82	6.54	5.7	-0.2
g	7	4	-41	-41	-40	-38	-37	-35	-34	-33	-31	-29	-40	-32	-32	-26	-22	-14	-12	-6	-1	5	9.1	12.30	14.00	15.0	0.1
h	7	4	-1	0	1	2	4	5	6	7	7	6	10	8	7	6	8	10	16	20	21	24	24.0	25.35	24.96	24.4	-0.3
g	7	5	-21	-20	-19	-18	-16	-14	-12	-11	-9	-10	-7	-11	-7	-6	-2	0	1	4	5	4	6.9	9.37	10.46	9.4	-0.6
h	7	5	28	28	28	28	28	29	29	29	29	28	36	28	23	26	23	22	18	17	17	17	14.8	10.93	7.03	3.4	-0.6
g	7	6	18	18	18	19	19	19	18	18	17	15	5	9	17	13	13	12	11	10	9	8	7.3	5.42	1.64	-2.8	-0.8
h	7	6	-12	-12	-13	-15	-16	-17	-18	-19	-20	-17	-18	-20	-18	-23	-23	-23	-23	-23	-23	-24	-25.4	-26.32	-27.61	-27.4	0.1

Table 3 12th Generation International Geomagnetic Reference Field *(Continued)*

g	7	7	6	6	6	6	6	6	6	6	5	29	19	18	8	1	-2	-5	-2	0	0	-2	-1.2	1.94	4.92	6.8	0.2
h	7	7	-22	-22	-22	-22	-22	-21	-20	-19	-19	-22	-16	-18	-17	-12	-11	-12	-10	-7	-4	-6	-5.8	-4.64	-3.28	-2.2	-0.2
g	8	0	11	11	11	11	11	11	11	11	11	13	22	11	15	13	14	14	18	21	23	25	24.4	24.80	24.41	24.2	0.2
g	8	1	8	8	8	8	7	7	7	7	7	7	15	9	6	5	6	6	6	6	5	6	6.6	7.62	8.21	8.8	0.0
h	8	1	8	8	8	8	8	8	8	8	8	12	5	10	11	7	7	6	7	8	10	11	11.9	11.20	10.84	10.1	-0.3
g	8	2	-4	-4	-4	-4	-3	-3	-3	-3	-3	-8	-4	-6	-4	-4	-2	-1	0	0	-1	-6	-9.2	-11.73	-14.50	-16.9	-0.6
h	8	2	-14	-15	-15	-15	-15	-15	-15	-15	-14	-21	-22	-15	-14	-12	-15	-16	-18	-19	-19	-21	-21.5	-20.88	-20.03	-18.3	0.3
g	8	3	-9	-9	-9	-9	-9	-9	-9	-9	-10	-5	-1	-14	-11	-14	-13	-12	-11	-11	-10	-9	-7.9	-6.88	-5.59	-3.2	0.5
h	8	3	7	7	6	6	6	6	5	5	5	-12	0	5	7	9	6	4	4	5	6	8	8.5	9.83	11.83	13.3	0.1
g	8	4	1	1	1	2	2	2	2	1	1	9	11	6	2	0	-3	-8	-7	-9	-12	-14	-16.6	-18.11	-19.34	-20.6	-0.2
h	8	4	-13	-13	-13	-13	-14	-14	-14	-15	-15	-7	-21	-23	-18	-16	-17	-19	-22	-23	-22	-23	-21.5	-19.71	-17.41	-14.6	0.5
g	8	5	2	2	2	3	4	4	5	6	6	7	15	10	10	8	5	4	4	4	3	9	9.1	10.17	11.61	13.4	0.4
h	8	5	5	5	5	5	5	5	5	5	5	2	-8	3	4	4	6	6	9	11	12	15	15.5	16.22	16.71	16.2	-0.2
g	8	6	-9	-8	-8	-8	-7	-7	-6	-6	-5	-10	-13	-7	-5	-1	0	0	3	4	4	6	7.0	9.36	10.85	11.7	0.1
h	8	6	16	16	16	16	17	17	18	18	19	18	17	23	23	24	21	18	16	14	12	11	8.9	7.61	6.96	5.7	-0.3
g	8	7	5	5	5	6	6	7	8	8	9	7	5	6	10	11	11	10	6	4	2	-5	-7.9	-11.25	-14.05	-15.9	-0.4
h	8	7	-5	-5	-5	-5	-5	-5	-5	-5	-5	3	-4	-4	1	-3	-6	-10	-13	-15	-16	-16	-14.9	-12.76	-10.74	-9.1	0.3
g	8	8	8	8	8	8	8	8	8	7	7	2	-1	9	8	4	3	1	-1	-4	-6	-7	-7.0	-4.87	-3.54	-2.0	0.3
h	8	8	-18	-18	-18	-18	-19	-19	-19	-19	-19	-11	-17	-13	-20	-17	-16	-17	-15	-11	-10	-4	-2.1	-0.06	1.64	2.1	0.0
g	9	0	8	8	8	8	8	8	8	8	8	5	3	4	4	8	8	7	5	5	4	4	5.0	5.58	5.50	5.4	-
g	9	1	10	10	10	10	10	10	10	10	10	-21	-7	9	6	10	10	10	10	10	9	9	9.4	9.76	9.45	8.8	-
h	9	1	-20	-20	-20	-20	-20	-20	-20	-20	-21	-27	-24	-11	-18	-22	-21	-21	-21	-21	-20	-20	-19.7	-20.11	-20.54	-21.6	-
g	9	2	1	1	1	1	1	1	1	1	1	1	-1	-4	0	2	2	2	1	1	1	3	3.0	3.58	3.45	3.1	-
h	9	2	14	14	14	14	14	14	14	15	15	17	19	12	12	15	16	16	16	15	15	15	13.4	12.69	11.51	10.8	-
g	9	3	-11	-11	-11	-11	-11	-11	-12	-12	-12	-11	-25	-5	-9	-13	-12	-12	-12	-12	-12	-10	-8.4	-6.94	-5.27	-3.3	-
h	9	3	5	5	5	5	5	5	5	5	5	29	12	7	2	7	6	7	9	9	11	12	12.5	12.67	12.75	11.8	-
g	9	4	12	12	12	12	12	12	12	11	11	3	10	2	1	10	10	10	9	9	9	8	6.3	5.01	3.13	0.7	-
h	9	4	-3	-3	-3	-3	-3	-3	-3	-3	-3	-9	2	6	0	-4	-4	-4	-5	-6	-7	-6	-6.2	-6.72	-7.14	-6.8	-
g	9	5	1	1	1	1	1	1	1	1	1	16	5	4	4	-1	-1	-1	-3	-3	-4	-8	-8.9	-10.76	-12.38	-13.3	-
h	9	5	-2	-2	-2	-2	-2	-2	-2	-3	-3	4	2	-2	-3	-5	-5	-5	-6	-6	-7	-8	-8.4	-8.16	-7.42	-6.9	-
g	9	6	-2	-2	-2	-2	-2	-2	-2	-2	-2	-3	-5	1	-1	-1	0	-1	-1	-1	-2	-1	-1.5	-1.25	-0.76	-0.1	-
h	9	6	8	8	8	8	9	9	9	9	9	9	8	10	9	10	10	10	9	9	9	8	8.4	8.10	7.97	7.8	-

Table 3 12th Generation International Geomagnetic Reference Field *(Continued)*

g	9	7	2	2	2	2	2	2	3	3	3	-4	-2	2	-2	5	3	4	7	7	7	10	9.3	8.76	8.43	8.7	-
h	9	7	10	10	10	10	10	10	10	11	11	6	8	7	8	10	11	11	10	9	8	5	3.8	2.92	2.14	1.0	-
g	9	8	-1	0	0	0	0	0	0	0	1	-3	3	2	3	1	1	1	2	1	1	-2	-4.3	-6.66	-8.42	-9.1	-
h	9	8	-2	-2	-2	-2	-2	-2	-2	-2	-2	1	-11	-6	0	-4	-2	-3	-6	-7	-7	-8	-8.2	-7.73	-6.08	-4.0	-
g	9	9	-1	-1	-1	-1	-1	-1	-2	-2	-2	-4	8	5	-1	-2	-1	-2	-5	-5	-6	-8	-8.2	-9.22	-10.08	-10.5	-
h	9	9	2	2	2	2	2	2	2	2	2	8	-7	5	5	1	1	1	2	2	2	3	4.8	6.01	7.01	8.4	-
g	10	0	-3	-3	-3	-3	-3	-3	-3	-3	-3	-3	-8	-3	1	-2	-3	-3	-4	-4	-3	-3	-2.6	-2.17	-1.94	-1.9	-
g	10	1	-4	-4	-4	-4	-4	-4	-4	-4	-4	11	4	-5	-3	-3	-3	-3	-4	-4	-4	-6	-6.0	-6.12	-6.24	-6.3	-
h	10	1	2	2	2	2	2	2	2	2	2	5	13	-4	4	2	1	1	1	1	2	1	1.7	2.19	2.73	3.2	-
g	10	2	2	2	2	2	2	2	2	2	2	1	-1	-1	4	2	2	2	2	3	2	2	1.7	1.42	0.89	0.1	-
h	10	2	1	1	1	1	1	1	1	1	1	1	-2	0	1	1	1	1	0	0	1	0	0.0	0.10	-0.10	-0.4	-
g	10	3	-5	-5	-5	-5	-5	-5	-5	-5	-5	2	13	2	0	-5	-5	-5	-5	-5	-5	-4	-3.1	-2.35	-1.07	0.5	-
h	10	3	2	2	2	2	2	2	2	2	2	-20	-10	-8	0	2	3	3	3	3	3	4	4.0	4.46	4.71	4.6	-
g	10	4	-2	-2	-2	-2	-2	-2	-2	-2	-2	-5	-4	-3	-1	-2	-1	-2	-2	-2	-2	-1	-0.5	-0.15	-0.16	-0.5	-
h	10	4	6	6	6	6	6	6	6	6	6	-1	2	-2	2	6	4	4	6	6	6	5	4.9	4.76	4.44	4.4	-
g	10	5	6	6	6	6	6	6	6	6	6	-1	4	7	4	4	6	5	5	5	4	4	3.7	3.06	2.45	1.8	-
h	10	5	-4	-4	-4	-4	-4	-4	-4	-4	-4	-6	-3	-4	-5	-4	-4	-4	-4	-4	-4	-5	-5.9	-6.58	-7.22	-7.9	-
g	10	6	4	4	4	4	4	4	4	4	4	8	12	4	6	4	4	4	3	3	3	2	1.0	0.29	-0.33	-0.7	-
h	10	6	0	0	0	0	0	0	0	0	0	6	6	1	1	0	0	-1	0	0	0	-1	-1.2	-1.01	-0.96	-0.6	-
g	10	7	0	0	0	0	0	0	0	0	0	-1	3	-2	1	0	1	1	1	1	1	2	2.0	2.06	2.13	2.1	-
h	10	7	-2	-2	-2	-2	-2	-2	-2	-1	-1	-4	-3	-3	-1	-2	-1	-1	-1	-1	-2	-2	-2.9	-3.47	-3.95	-4.2	-
g	10	8	2	2	2	1	1	1	1	2	2	-3	2	6	-1	2	0	0	2	2	3	5	4.2	3.77	3.09	2.4	-
h	10	8	4	4	4	4	4	4	4	4	4	-2	6	7	6	3	3	3	4	4	3	1	0.2	-0.86	-1.99	-2.8	-
g	10	9	2	2	2	2	3	3	3	3	3	5	10	-2	2	2	3	3	3	3	3	1	0.3	-0.21	-1.03	-1.8	-
h	10	9	0	0	0	0	0	0	0	0	0	0	11	-1	0	0	1	1	0	0	-1	-2	-2.2	-2.31	-1.97	-1.2	-
g	10	10	0	0	0	0	0	0	0	0	0	-2	3	0	0	0	-1	-1	0	0	0	0	-1.1	-2.09	-2.80	-3.6	-
h	10	10	-6	-6	-6	-6	-6	-6	-6	-6	-6	-2	8	-3	-7	-6	-4	-5	-6	-6	-6	-7	-7.4	-7.93	-8.31	-8.7	-
g	11	0	-	-	-	-	-	-	-	-	-	-	-	-	-	-	-	-	-	-	-	-	2.7	2.95	3.05	3.1	-
g	11	1	-	-	-	-	-	-	-	-	-	-	-	-	-	-	-	-	-	-	-	-	-1.7	-1.60	-1.48	-1.5	-
h	11	1	-	-	-	-	-	-	-	-	-	-	-	-	-	-	-	-	-	-	-	-	0.1	0.26	0.13	-0.1	-
g	11	2	-	-	-	-	-	-	-	-	-	-	-	-	-	-	-	-	-	-	-	-	-1.9	-1.88	-2.03	-2.3	-
h	11	2	-	-	-	-	-	-	-	-	-	-	-	-	-	-	-	-	-	-	-	-	1.3	1.44	1.67	2.0	-

Table 3 12th Generation International Geomagnetic Reference Field *(Continued)*

g	11	3	-	-	-	-	-	-	-	-	-	-	-	-	-	-	-	-	-	-	-	-	1.5	1.44	1.65	2.0	-
h	11	3	-	-	-	-	-	-	-	-	-	-	-	-	-	-	-	-	-	-	-	-	-0.9	-0.77	-0.66	-0.7	-
g	11	4	-	-	-	-	-	-	-	-	-	-	-	-	-	-	-	-	-	-	-	-	-0.1	-0.31	-0.51	-0.8	-
h	11	4	-	-	-	-	-	-	-	-	-	-	-	-	-	-	-	-	-	-	-	-	-2.6	-2.27	-1.76	-1.1	-
g	11	5	-	-	-	-	-	-	-	-	-	-	-	-	-	-	-	-	-	-	-	-	0.1	0.29	0.54	0.6	-
h	11	5	-	-	-	-	-	-	-	-	-	-	-	-	-	-	-	-	-	-	-	-	0.9	0.90	0.85	0.8	-
g	11	6	-	-	-	-	-	-	-	-	-	-	-	-	-	-	-	-	-	-	-	-	-0.7	-0.79	-0.79	-0.7	-
h	11	6	-	-	-	-	-	-	-	-	-	-	-	-	-	-	-	-	-	-	-	-	-0.7	-0.58	-0.39	-0.2	-
g	11	7	-	-	-	-	-	-	-	-	-	-	-	-	-	-	-	-	-	-	-	-	0.7	0.53	0.37	0.2	-
h	11	7	-	-	-	-	-	-	-	-	-	-	-	-	-	-	-	-	-	-	-	-	-2.8	-2.69	-2.51	-2.2	-
g	11	8	-	-	-	-	-	-	-	-	-	-	-	-	-	-	-	-	-	-	-	-	1.7	1.80	1.79	1.7	-
h	11	8	-	-	-	-	-	-	-	-	-	-	-	-	-	-	-	-	-	-	-	-	-0.9	-1.08	-1.27	-1.4	-
g	11	9	-	-	-	-	-	-	-	-	-	-	-	-	-	-	-	-	-	-	-	-	0.1	0.16	0.12	-0.2	-
h	11	9	-	-	-	-	-	-	-	-	-	-	-	-	-	-	-	-	-	-	-	-	-1.2	-1.58	-2.11	-2.5	-
g	11	10	-	-	-	-	-	-	-	-	-	-	-	-	-	-	-	-	-	-	-	-	1.2	0.96	0.75	0.4	-
h	11	10	-	-	-	-	-	-	-	-	-	-	-	-	-	-	-	-	-	-	-	-	-1.9	-1.90	-1.94	-2.0	-
g	11	11	-	-	-	-	-	-	-	-	-	-	-	-	-	-	-	-	-	-	-	-	4.0	3.99	3.75	3.5	-
h	11	11	-	-	-	-	-	-	-	-	-	-	-	-	-	-	-	-	-	-	-	-	-0.9	-1.39	-1.86	-2.4	-
g	12	0	-	-	-	-	-	-	-	-	-	-	-	-	-	-	-	-	-	-	-	-	-2.2	-2.15	-2.12	-1.9	-
g	12	1	-	-	-	-	-	-	-	-	-	-	-	-	-	-	-	-	-	-	-	-	-0.3	-0.29	-0.21	-0.2	-
h	12	1	-	-	-	-	-	-	-	-	-	-	-	-	-	-	-	-	-	-	-	-	-0.4	-0.55	-0.87	-1.1	-
g	12	2	-	-	-	-	-	-	-	-	-	-	-	-	-	-	-	-	-	-	-	-	0.2	0.21	0.30	0.4	-
h	12	2	-	-	-	-	-	-	-	-	-	-	-	-	-	-	-	-	-	-	-	-	0.3	0.23	0.27	0.4	-
g	12	3	-	-	-	-	-	-	-	-	-	-	-	-	-	-	-	-	-	-	-	-	0.9	0.89	1.04	1.2	-
h	12	3	-	-	-	-	-	-	-	-	-	-	-	-	-	-	-	-	-	-	-	-	2.5	2.38	2.13	1.9	-
g	12	4	-	-	-	-	-	-	-	-	-	-	-	-	-	-	-	-	-	-	-	-	-0.2	-0.38	-0.63	-0.8	-
h	12	4	-	-	-	-	-	-	-	-	-	-	-	-	-	-	-	-	-	-	-	-	-2.6	-2.63	-2.49	-2.2	-
g	12	5	-	-	-	-	-	-	-	-	-	-	-	-	-	-	-	-	-	-	-	-	0.9	0.96	0.95	0.9	-
h	12	5	-	-	-	-	-	-	-	-	-	-	-	-	-	-	-	-	-	-	-	-	0.7	0.61	0.49	0.3	-
g	12	6	-	-	-	-	-	-	-	-	-	-	-	-	-	-	-	-	-	-	-	-	-0.5	-0.30	-0.11	0.1	-
h	12	6	-	-	-	-	-	-	-	-	-	-	-	-	-	-	-	-	-	-	-	-	0.3	0.40	0.59	0.7	-
g	12	7	-	-	-	-	-	-	-	-	-	-	-	-	-	-	-	-	-	-	-	-	0.3	0.46	0.52	0.5	-

Table 3 12th Generation International Geomagnetic Reference Field *(Continued)*

h	12	7	-	-	-	-	-	-	-	-	-	-	-	-	-	-	-	-	-	-	-	-	0.0	0.01	0.00	-0.1	-
g	12	8	-	-	-	-	-	-	-	-	-	-	-	-	-	-	-	-	-	-	-	-	-0.3	-0.35	-0.39	-0.3	-
h	12	8	-	-	-	-	-	-	-	-	-	-	-	-	-	-	-	-	-	-	-	-	0.0	0.02	0.13	0.3	-
g	12	9	-	-	-	-	-	-	-	-	-	-	-	-	-	-	-	-	-	-	-	-	-0.4	-0.36	-0.37	-0.4	-
h	12	9	-	-	-	-	-	-	-	-	-	-	-	-	-	-	-	-	-	-	-	-	0.3	0.28	0.27	0.2	-
g	12	10	-	-	-	-	-	-	-	-	-	-	-	-	-	-	-	-	-	-	-	-	-0.1	0.08	0.21	0.2	-
h	12	10	-	-	-	-	-	-	-	-	-	-	-	-	-	-	-	-	-	-	-	-	-0.9	-0.87	-0.86	-0.9	-
g	12	11	-	-	-	-	-	-	-	-	-	-	-	-	-	-	-	-	-	-	-	-	-0.2	-0.49	-0.77	-0.9	-
h	12	11	-	-	-	-	-	-	-	-	-	-	-	-	-	-	-	-	-	-	-	-	-0.4	-0.34	-0.23	-0.1	-
g	12	12	-	-	-	-	-	-	-	-	-	-	-	-	-	-	-	-	-	-	-	-	-0.4	-0.08	0.04	0.0	-
h	12	12	-	-	-	-	-	-	-	-	-	-	-	-	-	-	-	-	-	-	-	-	0.8	0.88	0.87	0.7	-
g	13	0	-	-	-	-	-	-	-	-	-	-	-	-	-	-	-	-	-	-	-	-	-0.2	-0.16	-0.09	0.0	-
g	13	1	-	-	-	-	-	-	-	-	-	-	-	-	-	-	-	-	-	-	-	-	-0.9	-0.88	-0.89	-0.9	-
h	13	1	-	-	-	-	-	-	-	-	-	-	-	-	-	-	-	-	-	-	-	-	-0.9	-0.76	-0.87	-0.9	-
g	13	2	-	-	-	-	-	-	-	-	-	-	-	-	-	-	-	-	-	-	-	-	0.3	0.30	0.31	0.4	-
h	13	2	-	-	-	-	-	-	-	-	-	-	-	-	-	-	-	-	-	-	-	-	0.2	0.33	0.30	0.4	-
g	13	3	-	-	-	-	-	-	-	-	-	-	-	-	-	-	-	-	-	-	-	-	0.1	0.28	0.42	0.5	-
h	13	3	-	-	-	-	-	-	-	-	-	-	-	-	-	-	-	-	-	-	-	-	1.8	1.72	1.66	1.6	-
g	13	4	-	-	-	-	-	-	-	-	-	-	-	-	-	-	-	-	-	-	-	-	-0.4	-0.43	-0.45	-0.5	-
h	13	4	-	-	-	-	-	-	-	-	-	-	-	-	-	-	-	-	-	-	-	-	-0.4	-0.54	-0.59	-0.5	-
g	13	5	-	-	-	-	-	-	-	-	-	-	-	-	-	-	-	-	-	-	-	-	1.3	1.18	1.08	1.0	-
h	13	5	-	-	-	-	-	-	-	-	-	-	-	-	-	-	-	-	-	-	-	-	-1.0	-1.07	-1.14	-1.2	-
g	13	6	-	-	-	-	-	-	-	-	-	-	-	-	-	-	-	-	-	-	-	-	-0.4	-0.37	-0.31	-0.2	-
h	13	6	-	-	-	-	-	-	-	-	-	-	-	-	-	-	-	-	-	-	-	-	-0.1	-0.04	-0.07	-0.1	-
g	13	7	-	-	-	-	-	-	-	-	-	-	-	-	-	-	-	-	-	-	-	-	0.7	0.75	0.78	0.8	-
h	13	7	-	-	-	-	-	-	-	-	-	-	-	-	-	-	-	-	-	-	-	-	0.7	0.63	0.54	0.4	-
g	13	8	-	-	-	-	-	-	-	-	-	-	-	-	-	-	-	-	-	-	-	-	-0.4	-0.26	-0.18	-0.1	-
h	13	8	-	-	-	-	-	-	-	-	-	-	-	-	-	-	-	-	-	-	-	-	0.3	0.21	0.10	-0.1	-
g	13	9	-	-	-	-	-	-	-	-	-	-	-	-	-	-	-	-	-	-	-	-	0.3	0.35	0.38	0.3	-
h	13	9	-	-	-	-	-	-	-	-	-	-	-	-	-	-	-	-	-	-	-	-	0.6	0.53	0.49	0.4	-
g	13	10	-	-	-	-	-	-	-	-	-	-	-	-	-	-	-	-	-	-	-	-	-0.1	-0.05	0.02	0.1	-
h	13	10	-	-	-	-	-	-	-	-	-	-	-	-	-	-	-	-	-	-	-	-	0.3	0.38	0.44	0.5	-

Table 3 12th Generation International Geomagnetic Reference Field *(Continued)*

g	13	11	-	-	-	-	-	-	-	-	-	-	-	-	-	-	-	-	-	-	-	-	0.4	0.41	0.42	0.5	-
h	13	11	-	-	-	-	-	-	-	-	-	-	-	-	-	-	-	-	-	-	-	-	-0.2	-0.22	-0.25	-0.3	-
g	13	12	-	-	-	-	-	-	-	-	-	-	-	-	-	-	-	-	-	-	-	-	0.0	-0.10	-0.26	-0.4	-
h	13	12	-	-	-	-	-	-	-	-	-	-	-	-	-	-	-	-	-	-	-	-	-0.5	-0.57	-0.53	-0.4	-
g	13	13	-	-	-	-	-	-	-	-	-	-	-	-	-	-	-	-	-	-	-	-	0.1	-0.18	-0.26	-0.3	-
h	13	13	-	-	-	-	-	-	-	-	-	-	-	-	-	-	-	-	-	-	-	-	-0.9	-0.82	-0.79	-0.8	-

Here, Schmidt semi-normalized spherical harmonic coefficients are provided. Coefficients for degrees n=1-13 in units of nanotesla are listed for IGRF and definitive DGRF main-field models. Coefficients for degrees n=1-8 in units of nanotesla/year are listed for the predictive secular variation. Undefined coefficients are marked with '-'; these should be set to 0.0 in numerical calculations as is the case in the coefficient files available online.

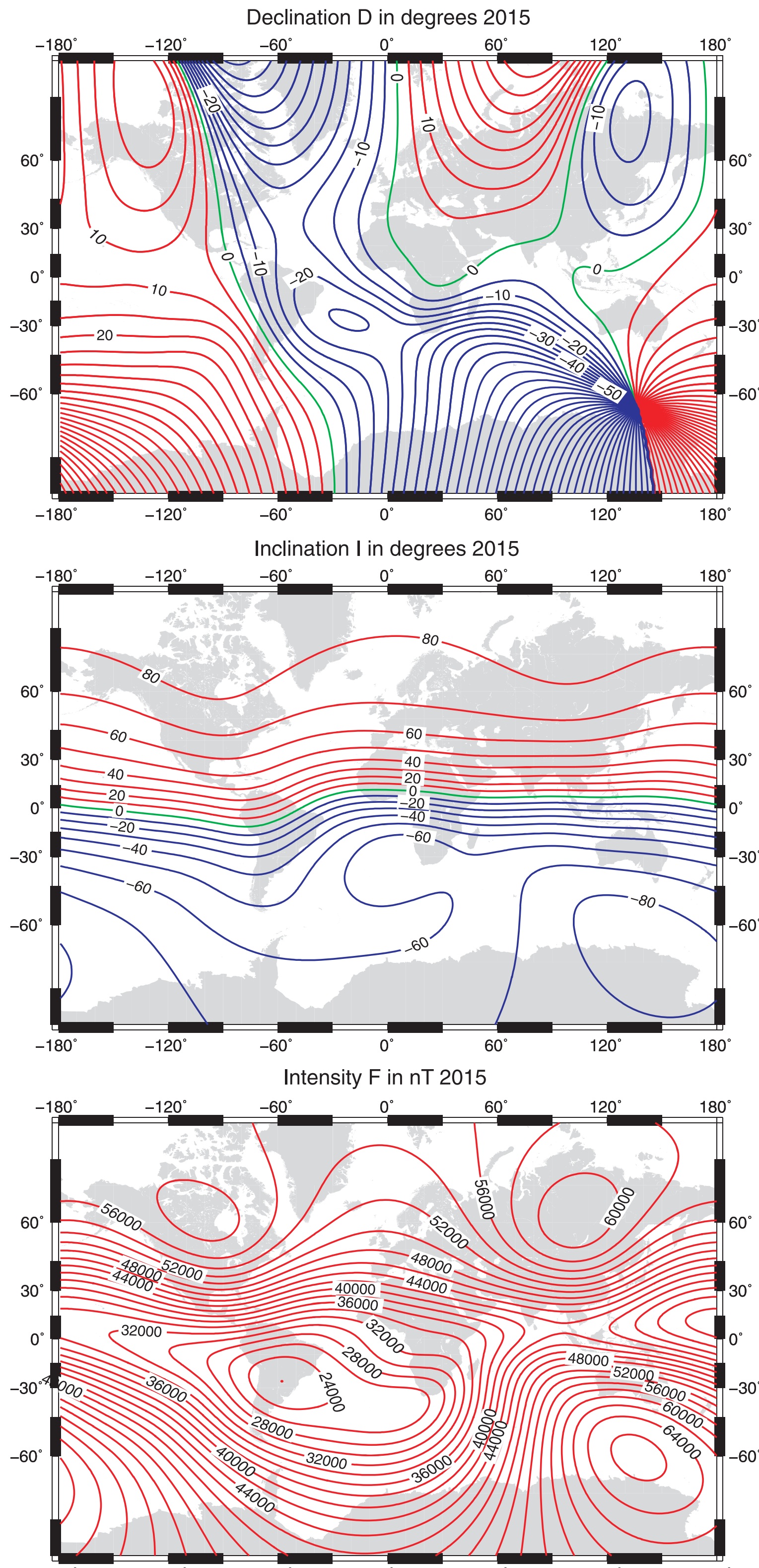

Figure 1 Maps of the magnetic declination D (top, units are degrees), inclination I (middle, units are degrees), and total intensity F (bottom, units are nT) at the Earth's mean radius $r = a$ in 2015; the red dot indicates the minimum intensity. Projection is Mercator.

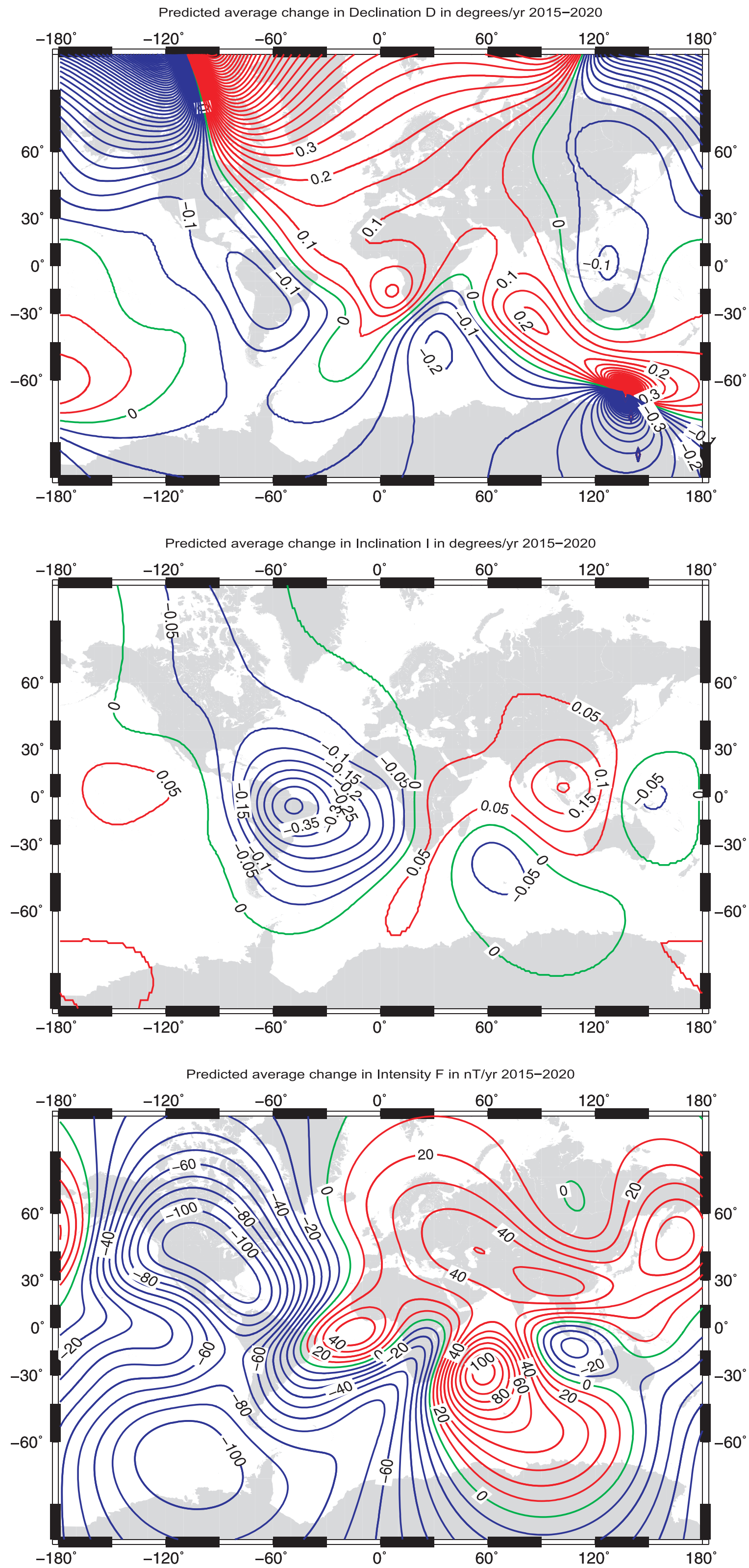

Figure 2 Maps of the predicted rate of change per year in the declination D (top, units are degrees/year), the inclination I (middle, units are degrees/year), and total intensity F (bottom, units are nT/year) at the Earth's mean radius $r = a$ for the interval 2015.0 to 2020.0. Projection is Mercator.

for the MF models and of nT/year for the predictive SV model. The coefficients are also available at http://www.ngdc.noaa.gov/IAGA/vmod/igrf.html, together with software to compute the magnetic field components at times and locations of interest, in both geodetic and geocentric reference frames. IGRF-12 is also available from the World Data Centers listed at the end of this paper.

We display in Figure 1 maps of the declination D, inclination I, and total intensity F in 2015.0 on the Earth's reference sphere ($r = a$) in a Mercator projection that is well suited to navigation. The green lines are the zero contours; in the declination map, the line shows the agonic line where true geographic and magnetic north/south as predicted by the model coincide on the Earth's surface. The general features shown by the maps in 2015 are well known (e.g., Finlay et al. 2010a) and have slowly evolved through the 115 years covered by IGRF-12. In particular, the minimum of magnetic intensity (see Figure 1 bottom), also known as the South Atlantic Anomaly, has continuously drifted westward and decreased since 1900. The point of minimum intensity at the Earth's surface is currently over Southern Paraguay and is expected to cross the political boundary with Argentina during the second half of 2016. Maps of the predictive annual rate of change for D, I, and F between 2015 and 2020 at the Earth's surface are shown in Figure 2. They are consistent with the continuation of the long-established westward drift and deepening of the South Atlantic Anomaly.

The positions of the geomagnetic poles and the magnetic dip poles in the northern and southern hemispheres, tabulated in Table 4, are presented in Figure 3 on the Earth's reference sphere. We recall that the geomagnetic poles are the points of intersection between the tilted axis of a central inclined magnetic dipole and the sphere of radius $a = 6,371.2$ km. Their positions, expressed in the geocentric co-ordinate system, are antipodal and can be

Table 4 Magnetic pole positions since 1900 as determined from IGRF-12 in WGS84 geodetic latitude

	North dip pole		South dip pole		North geomagnetic pole		South geomagnetic pole	
Epoch	**Latitude**	**Longitude**	**Latitude**	**Longitude**	**Latitude**	**Longitude**	**Latitude**	**Longitude**
1900.0	70.46	-96.19	-71.72	148.32	78.68	-68.79	-78.68	111.21
1905.0	70.66	-96.48	-71.46	148.55	78.68	-68.75	-78.68	111.25
1910.0	70.79	-96.72	-71.15	148.64	78.66	-68.72	-78.66	111.28
1915.0	71.03	-97.03	-70.80	148.54	78.64	-68.57	-78.64	111.43
1920.0	71.34	-97.39	-70.41	148.20	78.63	-68.38	-78.63	111.62
1925.0	71.79	-98.00	-69.99	147.63	78.62	-68.27	-78.62	111.73
1930.0	72.27	-98.69	-69.52	146.79	78.60	-68.26	-78.60	111.74
1935.0	72.80	-99.34	-69.06	145.77	78.57	-68.36	-78.57	111.64
1940.0	73.30	-99.87	-68.57	144.60	78.55	-68.51	-78.55	111.49
1945.0	73.93	-100.24	-68.15	144.44	78.55	-68.53	-78.55	111.47
1950.0	74.64	-100.86	-67.89	143.55	78.55	-68.85	-78.55	111.15
1955.0	75.18	-101.41	-67.19	141.50	78.54	-69.16	-78.54	110.84
1960.0	75.30	-101.03	-66.70	140.23	78.58	-69.47	-78.58	110.53
1965.0	75.63	-101.34	-66.33	139.53	78.60	-69.85	-78.60	110.15
1970.0	75.88	-100.98	-66.02	139.40	78.66	-70.18	-78.66	109.82
1975.0	76.15	-100.64	-65.74	139.52	78.76	-70.47	-78.76	109.53
1980.0	76.91	-101.68	-65.42	139.34	78.88	-70.76	-78.88	109.24
1985.0	77.40	-102.61	-65.13	139.18	79.04	-70.90	-79.04	109.10
1990.0	78.09	-103.68	-64.91	138.90	79.21	-71.13	-79.21	108.87
1995.0	79.09	-105.42	-64.79	138.76	79.39	-71.42	-79.39	108.58
2000.0	80.97	-109.64	-64.66	138.30	79.61	-71.57	-79.61	108.43
2005.0	83.19	-118.24	-64.55	137.85	79.82	-71.81	-79.82	108.19
2010.0	85.02	-132.84	-64.43	137.32	80.09	-72.21	-80.09	107.78
2015.0	86.29	-160.06	-64.28	136.59	80.37	-72.63	-80.37	107.37
2020.0	86.39	169.80	-64.11	135.76	80.65	-73.17	-80.65	106.83

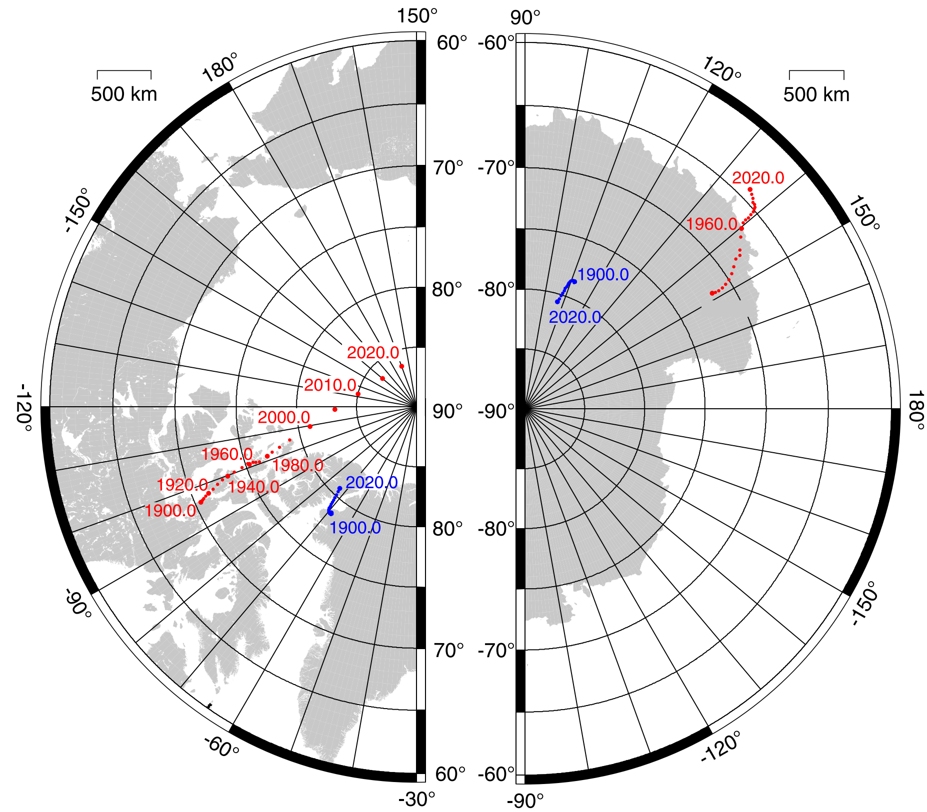

Figure 3 Motion of the magnetic dip pole (red) and geomagnetic pole (blue) since 1900 from IGRF-12 in the northern hemisphere (left) and the southern hemisphere (right). Stereographic projection is employed. The scale bar gives an indication of distance on the WGS84 ellipsoid that is correct along lines of constant longitude and also along the middle lines of latitude shown.

determined from only the three dipole ($n = 1$) Gauss coefficients. The magnetic dip poles are defined as the points on the Earth's surface where the magnetic field inclination, as determined from the entire field model to degree $n = N$, is vertical. They are referred to the north and south magnetic poles and are given in Table 4 for the field as observed in the geodetic WGS84 co-ordinate system. The comparison between the locations of the geomagnetic poles and the dip poles is of interest as, seen in the spherical frame, they would coincide if the Earth's magnetic field was perfectly dipolar. However, this is not the case. The comparison also illustrates the comparatively slower drift in time of the Earth's geomagnetic dipole compared to other contributions of the magnetic field. Interestingly, the movements of the north and south magnetic poles have not been erratic and have constantly moved northward since 1900. The tilt between the geomagnetic and the geographic axes is at present reducing with time; it is about 9.7° in 2015.0 and projected to be 9.4° in 2020. The north magnetic pole appeared to be accelerating rather smoothly over the last century (Figure 4) from about 5 to about 50 km/year with an increased acceleration around 1990 (Chulliat et al. 2010). The peculiar acceleration of the north and south magnetic poles between 1945 and 1955 as calculated by IGRF should be regarded with caution; see Xu (2000) for a discussion. Perhaps the most striking feature of IGRF-12 is that the north magnetic pole appears to have started a phase of deceleration with a velocity of about 53.2 km/year in 2015 and a projected velocity of 42.6 km/year in 2020. Note however that the later estimate relies on the predictive (SV) part of IGRF-12 for epoch 2015.0 to 2020.0 and that retrospective analysis has shown that errors could be significant (e.g., Finlay et al. 2010b). The locations computed from models are also intrinsically approximate due to the limited spatial resolution of the IGRF-12 models. For further details on the limitations of the IGRF for various applications and on difficulties in estimating its accuracy, readers should refer to Lowes (2000) or consult the IGRF 'Health Warning' found at http://www.ngdc.noaa.gov/IAGA/vmod/igrfhw.html.

IGRF-12 online data products

Further general information about the IGRF:
http://www.ngdc.noaa.gov/IAGA/vmod/igrf.html.
The coefficients of IGRF-12 in various file formats:
http://www.ngdc.noaa.gov/IAGA/vmod/igrf12coeffs.txt

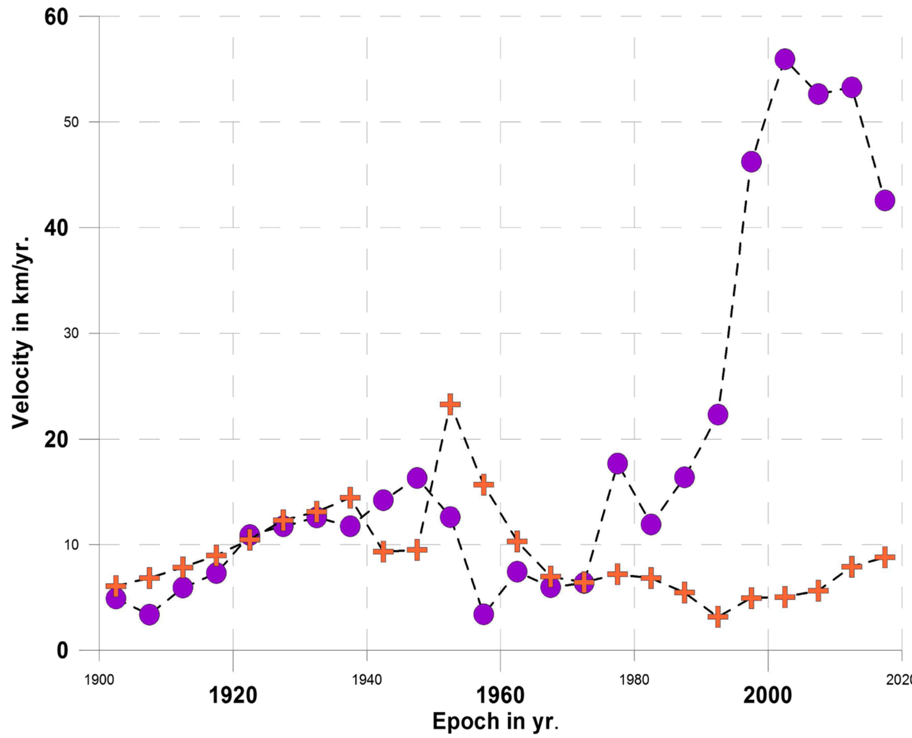

Figure 4 The northward velocity of the geomagnetic dip poles in the northern (purple dots) and southern (orange crosses) hemisphere as estimated by IGRF-12 on the WGS84 spheroid.

Fortran software for synthesizing the field from the coefficients:
http://www.ngdc.noaa.gov/IAGA/vmod/igrf12.f
C software for synthesizing the field from the coefficients (Linux):
http://www.ngdc.noaa.gov/IAGA/vmod/geomag70_linux.tar.gz
C software for synthesizing the field from the coefficients (Windows):
http://www.ngdc.noaa.gov/IAGA/vmod/geomag70_windows.zip
Online computation of field components from the IGRF-12 model:
http://www.ngdc.noaa.gov/geomag-web/?model=igrf
http://www.geomag.bgs.ac.uk/data_service/models_compass/igrf_form.shtml
http://wdc.kugi.kyoto-u.ac.jp/igrf/point/index.html
Archive of legacy versions of the IGRF model:
http://www.ngdc.noaa.gov/IAGA/vmod/igrf_old_models.html

Appendix: World Data Centers

WORLD DATA SERVICE FOR GEOPHYSICS, BOULDER
NOAA National Centers for Environmental Information, NOAA, 325 Broadway, E/GC, Boulder, CO 80305-3328
UNITED STATES OF AMERICA
INTERNET: http://www.ngdc.noaa.gov

WORLD DATA CENTRE FOR GEOMAGNETISM, COPENHAGEN
DTU Space, Diplomvej, Building 327, DK 2800, Kgs. Lynbgy, DENMARK
TEL: +45 4525 9713
FAX: +45 353 62475
EMAIL: cfinlay@space.dtu.dk
INTERNET: http://www.space.dtu.dk/English/Research/Scientific_data_and_models

WORLD DATA CENTRE FOR GEOMAGNETISM, EDINBURGH
British Geological Survey
Murchison House, West Mains Road
Edinburgh, EH9 3LA
UNITED KINGDOM
TEL: +44 131 650 0234
FAX: +44 131 668 4368
EMAIL: wdcgeomag@bgs.ac.uk
INTERNET: http://www.wdc.bgs.ac.uk/

WORLD DATA CENTRE FOR GEOMAGNETISM, KYOTO

Data Analysis Center for Geomagnetism and Space Magnetism
Graduate School of Science, Kyoto University
Kitashirakawa-Oiwake Cho, Sakyo-ku
Kyoto, 606-8502, JAPAN
TEL: +81 75 753 3929
FAX: +81 75 722 7884
EMAIL: iyemori@kugi.kyoto-u.ac.jp
INTERNET: http://wdc.kugi.kyoto-u.ac.jp

WORLD DATA CENTRE FOR GEOMAGNETISM, MUMBAI
Indian Institute of Geomagnetism
Colaba, Mumbai, 400 005, INDIA
TEL: +91 22 215 0293
FAX: +91 22 218 9568
EMAIL: abh@iigs.iigm.res.in
INTERNET: http://iigm.res.in

Competing interests
The authors declare that they have no competing interests.

Authors' contributions
ET and CCF coordinated the work with full support from the IGRF-12 task force members. CDB generated Figure 3 and verified with independent software the values given in Table 4. All authors participated to the construction of magnetic field candidate models referenced in the manuscript. All authors analyzed and discussed the final IGRF-12 model and approved the final version of the manuscript.

Authors' information
ET, CCF, CDB, PA, AD, GH, WK, VL, FJL, SM, NO, VP, and TJS are members of the IGRF-12 task force.

Acknowledgements
The institutes that support magnetic observatories together with INTERMAGNET are thanked for promoting high standards of observatory practice and prompt reporting. The support of the CHAMP mission by the German Aerospace Center (DLR) and the Federal Ministry of Education and Research is gratefully acknowledged. The Ørsted Project was made possible by extensive support from the Danish Government, NASA, ESA, CNES, DARA, and the Thomas B. Thriges Foundation. The authors also acknowledge ESA for providing access to the Swarm L1b data. E. Canet acknowledges the support of ESA through the Support to Science Element (STSE) program. This work was partly funded by the Centre National des Etudes Spatiales (CNES) within the context of the project of the 'Travaux préparatoires et exploitation de la mission Swarm.' W. Kuang and A. Tangborn were funded by NASA and the NSF. This work was partly supported by the French 'Agence Nationale de la Recherche' under the grant ANR-11-BS56-011 and by the Région Pays de Loire, France. I. Wardinski was supported by the DFG through SPP 1488. The IGRF-12 task force finally wishes to express their gratitude to C. Manoj and A. Woods for maintaining the IGRF web pages at NGDC. This is IPGP contribution no. 3625.

Author details
[1]Laboratoire de Planétologie et Géodynamique de Nantes, University of Nantes, UMR 6112 CNRS, 1 chemin de la Houssiniére F-44322, Nantes, France. [2]DTU Space, National Space Institute, Technical University of Denmark, Diplomvej 371, Lyngby, Denmark. [3]British Geological Survey, Murchison House, West Mains Road, EH9 3LA, Edinburgh, UK. [4]Cooperative Institute for Research in Environmental Sciences, University of Colorado, 216 UCB Boulder, CO 80309-0216, USA. [5]NOAA National Centers for Environmental Information (NCEI), 325 Broadway, E/GC, Boulder, CO 80305-3328, USA. [6]Institut de Physique du Globe de Paris, Sorbonne Paris Cité, Univ. Paris Diderot, CNRS, 1 rue Jussieu F-75005, Paris, France. [7]University Grenoble Alpes, ISTerre, CNRS, F-38041, Grenoble, France. [8]Université Grenoble Alpes, F-38000, Grenoble, France. [9]CEA, LETI, MINATEC Campus, F-38054, Grenoble, France. [10]Pushkov Institute of Terrestrial Magnetism, Ionosphere and Radio Wave Propagation, IZMIRAN, Kaluzhskoe Hwy 4, Troitsk, Moscow, Russia. [11]ETH Zürich Institut für Geophysik, Earth and Planetary Magnetism Group, Sonneggstrasse 58092 Zürich, Switzerland. [12]Institut de Physique du Globe de Strasbourg, UMR 7516-CNRS, Université de Strasbourg/EOST, Strasbourg, France. [13]Key Laboratory of Earth and Planetary Physics, Institute of Geology and Geophysics, Chinese Academy of Sciences 100029, Beijing, China. [14]Centre National d'Etudes Spatiales, 8 Avenue Edouard Belin, F-31400 Toulouse, France. [15]GFZ German Research Centre for Geosciences, Telegrafenberg, 14473 Potsdam Germany. [16]Planetary Geodynamics Laboratory, NASA GSFC, Greenbelt MD, USA. [17]School of Chemistry, University of Newcastle upon Tyne, NE1 7RU, Newcastle, UK. [18]CNES, Centre National d'Etudes Spatiales, 2 Place Maurice Quentin F-75001, Paris, France. [19]Départment de Géophysique USTHB, University of Algiers, PB 32 El-Alia Bab-Ezzouar, Algiers, Algeria. [20]Joint Center for Earth Systems Technology, UMBC, Baltimore, USA.

Received: 30 January 2015 Accepted: 13 April 2015
Published online: 27 May 2015

References
Alken P, Maus S, Chulliat A, Manoj C (2015) NOAA/NGDC candidate models for the 12th Generation International Geomagnetic Reference Field. Earth Planets Space 2015 67:68. doi:10.1186/s40623-015-0215-1
Barraclough DR (1987) International Geomagnetic Reference Field: the fourth generation. Phys Earth planet Int 48:279–292
Barton CE (1997) International Geomagnetic Reference Field: the seventh generation. J Geomag Geoelect 49:123–148
Chulliat A, Hulot G, Newitt LR (2010) Magnetic flux expulsion from the core as a possible cause of the unusually large acceleration of the north magnetic pole during the 1990s. J Geophys Res. 115, B07101, doi:10.1029/2009JB007143
Finlay CC, Maus S, Beggan CD, Bondar TN, Chambodut A, Chernova TA, Chulliat A, Golovkov VP, Hamilton B, Hamoudi M, Holme R, Hulot G, Kuang W, Langlais B, Lesur V, Lowes FJ, Lühr H, Macmillan S, Mandea M, McLean S, Manoj C, Menvielle M, Michaelis I, Olsen N, Rauberg J, Rother M, Sabaka TJ, Tangborn A, Tøffner-Clausen L, Thébault E, et al. (2010a) International Geomagnetic Reference Field: the eleventh generation. Geophys J Int 183(3):1216–1230. doi:10.1111/j.1365-246X.2010.04804.x.
Finlay CC, Maus S, Beggan CD, Hamoudi M, Lesur V, Lowes FJ, Olsen N, Thébault E (2010b) Evaluation of candidate geomagnetic field models for IGRF-11. Earth Planets Space IGRF Special issue 62(10):787–804
Finlay CC, Olsen N, Tøffner-Clausen L (2015) DTU candidate field models for IGRF-12 and the CHAOS-5 geomagnetic field model. Earth Planets Space, in press
Fournier A, Aubert J, Thébault E (2015) A candidate secular variation model for IGRF-12 based on Swarm data and inverse geodynamo modelling. Earth Planets and Space 67:81. doi:10.1186/s40623-015-0245-8
Gillet N, Barrois O, Finlay CC (2015) Stochastic forecasting of the geomagnetic field from the COV-OBS.x1 geomagnetic field model and candidate models for IGRF-12. Earth, Planets and Space 2015 67:71. doi:10.1186/s40623-015-0225-z
Hamilton B, Ridley VA, Beggan CD, Macmillan S (2015) The BGS magnetic field candidate models for the 12th generation IGRF. Earth, Planets and Space 2015 67:69. doi:10.1186/s40623-015-0227-x
Hamoudi M, Thébault E, Lesur V, Mandea M (2007) GeoForschungsZentrum Anomaly Magnetic MAp (GAMMA): a candidate model for the world digital magnetic anomaly map. Geochem Geophysics Geosystems 8(6)
Hemant K, Thébault E, Mandea M, Ravat D, Maus S (2007) Magnetic anomaly map of the world: merging satellite, airborne, marine and ground-based magnetic data sets. Earth Planet Sci Lett 260(1):56–71
Hulot G, Olsen N, Sabaka TJ (2007) The present field, geomagnetism. In: Schubert G (ed). Treatise on Geophysics, vol 5. Elsevier, Amsterdam. pp 33–75
IAGA Division I Study Group Geomagnetic Reference Fields (1975) International Geomagnetic Reference Field 1975. J Geomag Geoelect 27:437–439
Langel RA, Estes RH (1982) A geomagnetic field spectrum. Geophys Res Lett 9.4:250–253
Langel RA, Barraclough DR, Kerridge DJ, Golovkov VP, Sabaka TJ, Estes RH (1988) Definitive IGRF models for 1945, 1950, 1955, and 1960. J Geomag Geoelect 40:645–702

Langel RA (1992) International Geomagnetic Reference Field: the sixth generation. J Geomag Geoelect 44:679–707
Léger JM, Jager T, Bertrand F, Hulot G, Brocco L, Vigneron P, Lalanne X, Chulliat A, Fratter I (2015) In-flight performances of the absolute scalar magnetometer vector mode on board the Swarm satellites. Earth Planets and Space 57(25 April 2015):67
Lesur V, Rother M, Wardinski I, Schachtschneider R, Hamoudi M, Chambodut A (2015) Parent magnetic field models for the IGRF-12 GFZ-candidates. Earth Planets Space, in press
Lowes FJ (2000) An estimate of the errors of the IGRF/DGRF fields 1945–2000. Earth Planets Space 52(12):1207–1211
Macmillan S, Maus S, Bondar T, Chambodut A, Golovkov V, Holme R, Langlais B, Lesur V, Lowes FJ, Lühr H, Mai W, Mandea M, Olsen N, Rother M, Sabaka TJ, Thomson A, Wardinski I (2003) The 9th-Generation International Geomagnetic Reference Field. Geophys J Int 155:1051–1056
Mandea M, Macmillan S (2000) International Geomagnetic Reference Field - the eighth generation, 2000. Earth Planets Space 52:1119–1124
Maus S, Macmillan S, Chernova T, Choi S, Dater D, Golovkov V, Lesur V, Lowes FJ, Lühr H, Mai W, McLean S, Olsen N, Rother M, Sabaka TJ, Thomson A, Zvereva T (2005) The 10th-generation International Geomagnetic Reference Field. Geophys J Int 161:561–565
Maus S, Sazonova T, Hemant K, Fairhead JD, Ravat D (2007) National geophysical data center candidate for the world digital magnetic anomaly map. Geochem Geophys Geosyst 8(6):Q06017. doi:10.1029/2007GC001643
Neubert T, Mandea M, Hulot G, von Frese R, Primdahl F, Jørgensen JL, Friis-Christensen E, Stauning P, Olsen N, Risbo T (2001) Ørsted satellite captures high-precision geomagnetic field data, EOS. Trans Am. Geophys Un 82:81
Peddie NW (1982) International Geomagnetic Reference Field: the third generation. J Geomagn Geoelect 34:309–326
Reigber C, Lühr H, Schwintzer P (2002) CHAMP mission status. Adv Space Res 30:129–134
Saturnino D, Civet F, Langlais B, Thébault E, Mandea M (2015) Main field and secular variation candidate models for the 12th IGRF generation after 10 months of Swarm measurements, Earth, Planets and Space, in press
Thébault E, Finlay CC, Alken P, Beggan CD, Canet E, Chulliat A, Langlais B, Lesur V, Lowes FJ, Manoj C, Rother M, Schachtschneider R (2015) Evaluation of candidate geomagnetic field models for IGRF-12. Earth Planets Space, in press
Vigneron P, Hulot G, Olsen N, Léger JM, Jager T, Brocco L, Sirol O, Coïsson P, Lalanne X, Chulliat A, Bertrand F, Boness A, Fratter I (2015) A 2015 International Geomagnetic Reference Field (IGRF) candidate model based on Swarm's experimental absolute magnetometer vector mode data. Earth Planets Space, in press
Xu WY (2000) Unusual behaviour of the IGRF during the1945–1955 period. Earth Planets Space 52:1227–1233
Zmuda AJ (1971) The International Geomagnetic Reference Field: introduction. Bull Int Assoc Geomag Aeronomy 28:148–152